Clays and Clay Minerals, Vol. 42, No. 6, 689–701, 1994.

BIOGENIC NONTRONITE FROM MARINE WHITE SMOKER CHIMNEYS

BIRGIT KÖHLER,[1] ARIEH SINGER,[2] AND PETER STOFFERS[1]

[1] Geologisch-Paläontologisches Institut und Museum, Christian-Albrechts-Universität 24118 Kiel, Germany

[2] Department of Soil and Water Sciences, The Hebrew University of Jerusalem P.O. Box 12, Rehovot, 76-100, Israel

Abstract—Clay samples of greenish colour were collected from submarine hydrothermal chimneys of the Galapagos Rift and Mariana Trough. Mineralogical and chemical investigations of the clay by scanning and transmission electron microscopy, X-ray diffraction, differential thermal analysis, infrared-spectroscopy, X-ray fluorescence, and determination of specific surface area, and oxygen isotope composition identify it as a well crystallized nontronite. This nontronite of hydrothermal origin has a nearly monomineralic character, a low Al-content, and a formation temperature of 21.5 to 67.3°C. The most remarkable characteristic, however, of the nontronite deposit is its microstructure, a network of microtubes composed of fine frequently folded clay sheets. These delicate filaments show close similarity in size and form to sheath forming bacteria. The correlation between clay mineral and chemical characteristics, as well as biological conditions at marine hydrothermal smoker chimneys, let us suggest that Fe oxidizing, sheath forming bacteria are playing a decisive role in nontronite formation at these sites.

Key Words—Authigenic formation, Bio-catalysis, Hydrothermal, Microstructure, Nontronite, Scanning electron microscopy, Silicate smoker chimney.

INTRODUCTION

Deep-sea hydrothermal vents were discovered in 1977 along the Galapagos Rift, a part of the globe-encircling system of sea-floor spreading axes (Weiss *et al* 1977; Corliss *et al* 1979). Many hydrothermal fields have since been identified along the ridges of the East Pacific Rise and other sea-floor spreading sites (Rona 1984).

The vent solutions frequently give rise to precipitates that form chimneys of up to 10 m height and 50 cm diameter (e.g., Edmond *et al* 1982; Spiess *et al* 1980). With precipitates dominated by black sulfides these chimneys are called "black smokers." They are characterized by hot vent solutions (about 350° ± 30°C) with flow velocities of m s^{-1}. The vent solutions of "white smokers" have a lighter color due to the presence of relatively high concentrations of Ca-sulfates and colloidal silica. Less hot (270°C to 350°C) to warm (<100°C) solutions are emitted from these vents with flow velocities of cm s^{-1} (e.g., MacDonald *et al* 1980; Haymon and Kastner 1981; Haymon and MacDonald 1985; Von Damm 1990). Commonly the chimneys appear as groups or colonies on slight elevations or "mounds," which are composed of vent precipitates and debris of disintegrated chimneys. The lifetime of a smoker is limited, commonly not exceeding a few tens of years (Tunnicliffe and Juniper 1990).

The precipitates that build the chimney vary in relation to the composition and temperature of the hydrothermal solutions, and to parameters that determine the rate of their dilution in sea water. These variations, often cyclical in nature, have been described in detail for black smokers (e.g., Haymon 1983; Haymon and MacDonald 1985; von Damm 1990; Haymon *et al* 1993). At white smokers the vent solutions contain in addition to Fe, Mn and S, substantial concentrations of Si. With the exit of these solutions, all Fe, precipitates as sulfides, and only Mn-oxides precipitate subsequently. With a ratio $Fe/H_2S < 1$ in the vent solution, initially all Fe, precipitates as sulfides, and only Mn-oxides precipitate subsequently. With $Fe/H_2S > 1$, both Fe- and Mn-oxides precipitate (Edmond *et al* 1979) with Fe oxides closer to the vent exit. Silica precipitates intermittently, commonly in the form of opal A (Juniper and Fouquet 1988). This indicates that white smoker chimneys are essentially composed of Ca-sulfates, Fe- and Mn-oxides, accompanied by amorphous silica, in contrast to black smoker chimneys where sulfides are dominating.

Hydrothermal nontronite formation has been studied intensively in the Red Sea (Bischoff 1972; Cole and Shaw 1983; Cole 1983). Nontronite in these deposits, which are very recent (<25,000 Ma), has been found to occur both in association with sulfides and iron rich amorphous material (the "sulphide/silicate/amorphous facies") in an anoxic environment, and in association with poorly crystallized Fe^{3+} oxides and manganosiderite (the "silicate/carbonate/oxide facies") in oxic environments. In both environments, the

Table 1. Locations of the sample sites.

Sample	Position		Water-depth (m)
	Latitude	Longitude	
Galapagos Rift			
SO 32/179	0°46 10'N	85°54 90'W	2580
SO 39/181	0°46 04'N	85°54 62'W	2529
SO 39/188	0°46 10'N	85°55 10'W	2535
Mariana-Trough			
SO 57/18	18°12 78'N	144°42 51'E	3614
SO 57/19	18°12 86'N	144°42 46'E	3607

formation of the nontronite is thought to occur by sorption of silica supplied by the incoming hydrothermal brines onto Fe-oxyhydroxide, which settled from the upper brine pool layers. Poorly crystalline iron hydroxides, associated with nontronite in the upper part of a sediment column from the Atlantis II Deep (Red Sea), were proposed as precursor minerals for nontronite (Singer and Stoffers 1987). Conditions were assumed to have been oxic in this environment. Following the earlier work of Bischoff (1972), Badaut *et al* (1985, 1990, 1992) proposed that the first iron-rich smectite formed is ferrous-tri-octahedral, and that it quickly oxidizes to a ferric form, releasing free iron. Under higher redox conditions a nontronite is formed in intimate association with hisingeritic and with poorly-ordered iron precipitates (ferrihydrite or feroxyhyte). Due to this association it appears that the nontronite is formed from the compounds.

Oxygen isotopic investigations (McMurtry *et al* 1983; Cole 1983; Singer *et al* 1984) indicate that authigenic nontronites have formation temperatures of 30°C to 150°C. This large temperature range, combined with variability of redox conditions, raised questions about the chemical processes involved in their genesis. Most of the studies suggested processes of direct precipitation from hydrothermal fluids and combination of Fe-oxyhydroxides with hydrothermal (or biogenic) silica under more or less anoxic conditions (Heath and Dymond 1977; Cole and Shaw 1983; Cole 1985). Based on synthesis experiments, Harder (1976, 1978) concluded that Fe-smectites could only form from solutions containing Fe^{2+} and/or Mg^{2+}. In a series of experimental studies, Decarreau and Bonnin (1986) showed that the synthesis of ferric smectites could be carried out at relatively low temperatures (75°C) by aging coprecipitated gels of silica and Fe^{2+} sulphate under initially reducing, then oxidizing conditions. Under strictly reducing conditions only nuclei of a tri-octahedral ferrous stevensite were observed and crystal growth did not take place. When a spontaneous oxidation, in contact with air, was effected, the ferrous smectite nuclei transformed rapidly into a ferric, nontronite-like smectite. In a later study, Decarreau *et al* (1987) showed that the crystallization of a di-octahedral smectite, containing only Fe^{3+} in the octahedral sheet is also possible under strictly oxidizing conditions. Crystal growth, however, under these conditions is slow and goes to completion only at sufficiently high temperatures. Thus, the study of natural occurrences (particularly in the Red Sea) as well as synthesis experiments suggest that hydrothermal nontronite is likely formed in initially reducing conditions, with Fe principally in the ferrous state, and then oxidizing conditions (Decarreau *et al* 1987).

Based on the numerous reports on clay mineral formation at deep hydrothermal sites (see review in Chamley 1989) and on the first reports on nontronite formation on smokers (e.g., Köhler 1991; Köhler and Singer 1992), the objective of this study was to identify and characterize authigenic clay minerals, formed at some white smoker chimneys (Galapagos Rift and Mariana Trough).

SAMPLING LOCATIONS AND MATERIALS

Hydrothermal clay samples from white smoker chimneys were collected with TV-controlled grabs on expeditions of the research vessel "Sonne" to the Galapagos Rift (1984, 1985) and to the backarc Mariana Trough (1988). The locations of the samples are given in Table 1. Yellowgreen to dark green clay was attached to the outer wall of the silicate material of the smoker chimneys and to the upper inner wall of the vent channel. The thickness of this clay layer varies from 1 mm to several cm. A thin Fe-oxide crust occasionally exists between the silicate material and the nontronite layer.

All clay samples from the Galapagos Rift are of bright olive green color and have a loose, soft consistency. The color of the clay material of the Mariana Trough varies from weak olive brown (SO 57/18) to more yellowish green (SO 57/19). The consistency is more grainy. The associated chimney material consisted of a porous, brittle, yellowish to brownish silicate-rich precipitate, partly coated with Fe-oxides. Stoffers *et al* (1989) described this material as opal, aragonite and Mn,Fe-hydroxides. The chimney material of sample SO 57/19 contained in addition sulfides (pyrite, marcasite), barite, and alumite.

METHODS

After selections based on preliminary X-ray diffraction (XRD), the dispersed, Na-saturated, material was washed with distilled water until free of salts, as tested with $AgNO_3$. The fraction <2 μm was separated by sedimentation under thermoconstant conditions (22°C) Most analyses were carried out with Mg-saturated, freeze-dried subsamples of the fraction <2 μm. For X-ray diffraction (XRD) analysis, a Phillips PW 1710 diffractometer with Co-radiation, graphite monochrometer, and automatic divergence slit was used. The

XRD analyses were done on unoriented specimens and with oriented air-dried, glycolated and heated (520°C, 2 h) specimens.

Differential thermal analysis (DTA) was performed on a Perkin Elmer Model 1700 System 4 apparatus. For analysis 30 mg of material (<2 μm fraction), equilibrated at 58% RH, were heated at a rate of 10°C min^{-1}. Infrared spectroscopy (IRS) was carried out on a Nicolette FTIR apparatus. For analysis, KBr-disks were used. For transmission electron microscopy (TEM), a JEM 100 CX apparatus was used. Na-saturated, freeze-dried, suspensions were taken for analysis.

For scanning electron microscopy (SEM), principally a Cambridge S 150 instrument with attached EDAX element analyser was used. A part of the original undisturbed clay sample without any other pretreatment was dried and coated with carbon for analysis. Much attention was paid to the methodology of preparation of the samples. The methods of preparation tested included (a) air-drying at 20°C, (b) freeze-drying, and (c) replacement of porewater with a mixture of ethanol with acrylic resin, followed by heat hardening. The latter method was discarded because distinct structural changes occurred caused by shrinkage. Drying in air and freeze-drying caused the appearance of some salt efflorescences, but they were negligible. Freeze-drying was preferred because the original structures appeared to be preserved, while air-drying tended to cause rolling and aggregating of clay particles.

Chemical composition was determined by X-ray fluorescence analysis on a Philips XR spectrometer using a rhodium tube and an attached Philips PH computer. To determine the concentration of the major elements samples were fused with Spectromelt A 12 by Merck (66/34 (w/w) di-lithiumtetraborate/lithium-metaborate), while for trace elements Elaviz 55 was used. For specific surface area determinations, the ethylene-glycol-monoethylene (EGME) method (Carter *et al* 1965) was used.

Oxygen isotope determinations were carried out on clay material from which opaline material had been separated manually under the microscope. Free Fe- and Mn-oxides had been removed by the method of Mehra and Jackson (1960). Oxygen was extracted from silica samples by fluorination with ClF_3 (Borthwick and Harmon 1982) after heating the samples for 4 h at 150°C for dehydration. The precipitation temperatures of the clay material can be calculated using the equation for the smectite/water equilibrium $1000 \cdot \ln \alpha = 2.67 \cdot 10^6/T^2 - 4.82$ (T in °K) (Yeh and Savin 1977). For the opaline material, the minimum isotopic temperature is calculated using the equation $1000 \cdot \ln \alpha = 3.09 \cdot 10^6/T^2 - 3.29$ (Knauth and Epstein 1976), and for the maximum temperature the equation $1000 \cdot \ln \alpha = 3.38 \cdot 10^6/T^2 - 3.40$ (Clayton *et al* 1972). In these calculations, we assumed that the $\delta^{18}O$ composition of the vent water was 0‰.

RESULTS

The most notable feature of the white smoker chimney clays was their micromorphology. Scanning microscopy data will therefore be presented first.

Scanning electron microscopy (SEM)

Galapagos rift. The greenish samples SO 32/179, SO 39/181 and SO 39/188 displayed a sponge-like basic structure with a high porosity (Figure 1a). In the voids (pores) at high magnifications, aggregates of tube-like structures could be discerned that were attached to the channel walls and extended towards the void center (Figure 1b). The diameter of these tubes was 2.5 ± 0.5 μm, with a wall thickness of 1 ± 0.2 μm. The diameter of the inner cavity was 1 ± 0.2 μm. The length of the microtubes was difficult to measure, but it commonly exceeded 10 μm. In some areas, intergrowth of the microtubes had started, so that at fracture surfaces only a network of intertwining rills with a width of 1–1.2 μm could be discerned (Figures 1c and 1d). All sizes are taken from SEM-photographs. Under highest magnification, the microtubes could be seen to be composed of fine, frequently folded clay sheets. Chemical analyses by EDAX showed the predominance of Si and Fe, with only minor amounts of Mg and K. No qualitative chemical differences could be seen between the clay minerals forming the well shaped microtubes and those filling the interspaces (e.g., Figures 1c and 1d). In sample SO 32/179 the microtubes were particularly well-developed. In samples SO 39/181 and SO 39/188, variability was larger with well-developed microtube groups alongside.

Mariana trough. The microstructures from this site exhibited many of the characteristics of the Galapagos site. In sample SO 57/18 the (micro)structure was very open, loose, sometimes of a net-like character. Microtubes, with a width of 1.9 ± 0.3 μm and a length of over 10 μm grew in all directions from the substrates into the voids. The submicrostructure of the micropores consisted, as in the Galapagos site samples, of folded clay sheets composed of Si and Fe with traces of Mg, Ca and K (Figure 2). The clay material in sample SO 57/19 was more heterogeneous. It appeared at some parts in form of open, net-like aggregates, elongated, inflated or rounded. The microtubes that grew inward into the pore voids were curved or spiral-turned, with a total width of 2.9 ± 0.5 μm. The clay particles were concentrically arranged. In well-preserved portions, they were rolled in but enmeshed the tubes with sheets or thin bands (Figures 1e and 1f).

X-ray diffraction (XRD)

Galapagos rift. The bulk samples SO 32/179, SO 39/181 and SO 39/188 had a very similar mineralogy that

https://doi.org/10.1346/CCMN.1994.0420605 Published online by Cambridge University Press

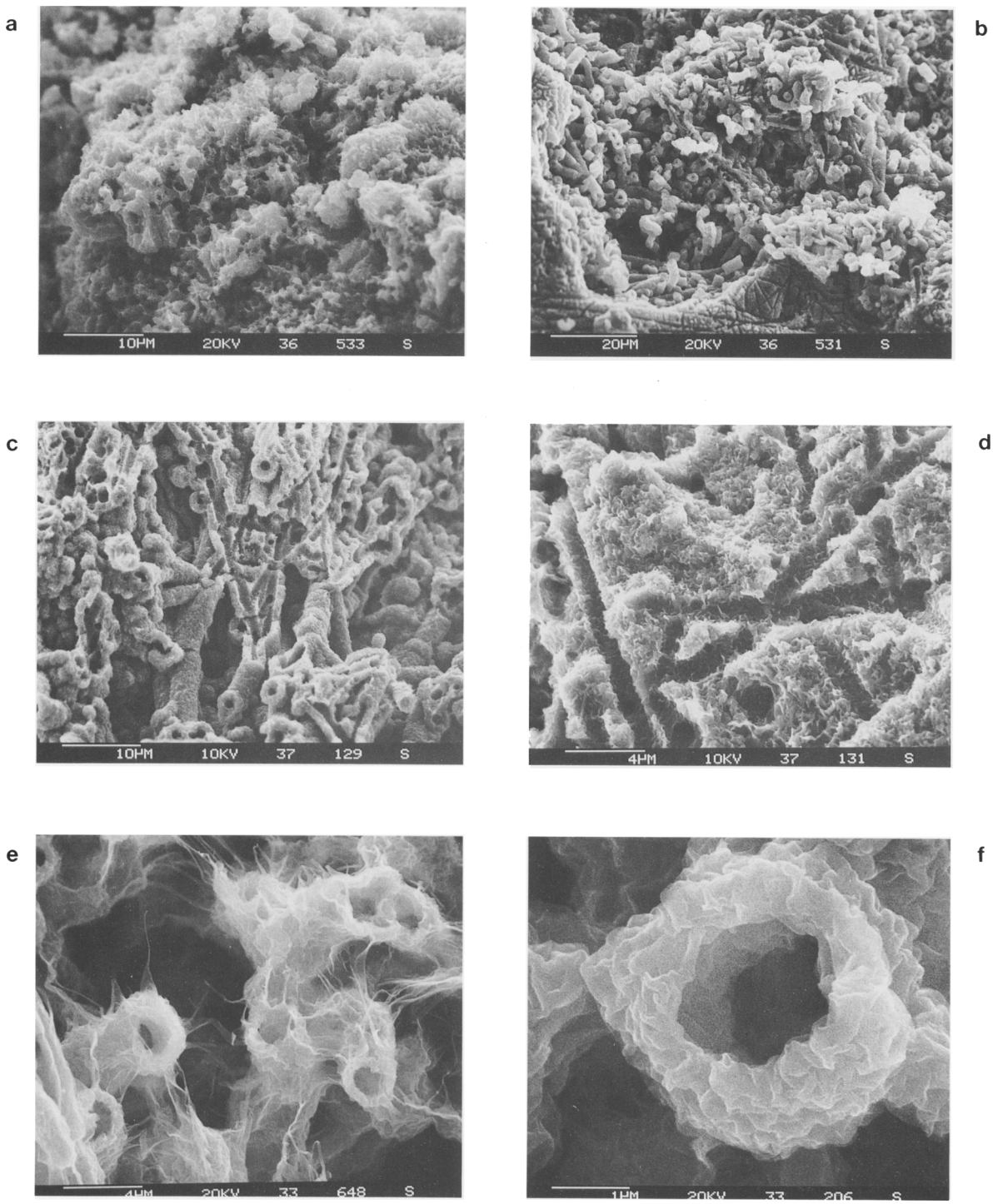

Figure 1. Micromorphology of the chimney clay from Galapagos Rift and Mariana Trough. a) sponge-like basic structure; b) filamentous microtubes; c) and d) network of intertwining rills; e) microtubes; f) microtube opening.

consisted almost monomineralically of smectite with traces of opal. The smectite in the clay fraction of these samples appeared to be fairly crystalline, with full expansion to 17 Å after glycol saturation. A 060 spacing of 1.516–1.518 Å indicated that they are dioctahedral smectites (Figure 3).

Mariana trough. The bulk samples had a very similar

https://doi.org/10.1346/CCMN.1994.0420605 Published online by Cambridge University Press

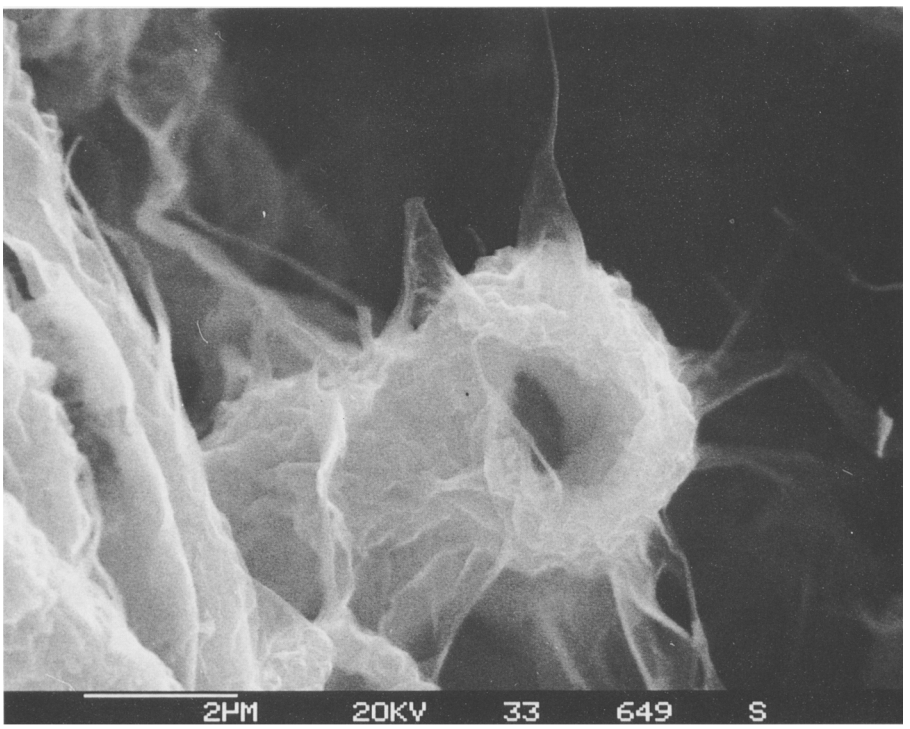

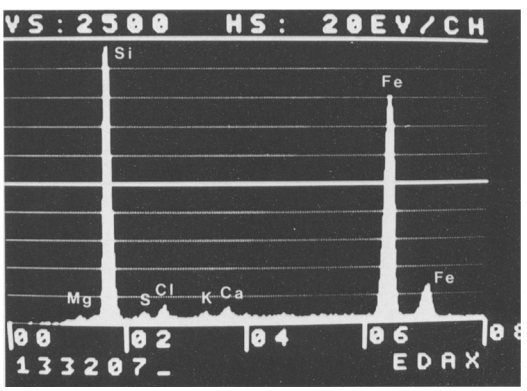

Figure 2. Nontronite microtube and EDAX-analysis.

composition dominated by smectite. In some samples traces of opal were present too. All smectites were dioctahedral, with a 060 spacing between 1.511 and 1.518 Å (Figure 3).

Differential thermal analysis (DTA)

The thermograms of all smectite clays displayed similar features (Figure 4); a very large low-temperature dehydration endotherm, a smaller dehydroxylation endotherm, and a weak high-temperature exotherm. The low-temperature dehydration endotherms took place between 120°C and 134°C. The most striking feature of the thermographs are the very low dehydroxylation endotherms. In the Galapagos Rift clays, they range between 434°C and 441°C, in the Mariana Trough clays between 446°C and 452°C. The weak exothermic reaction took place in the temperature range of 816°–848°C in the Galapagos clays and 852°C and 863°C in the Mariana Trough clays.

Infrared spectroscopy (IR)

The clay from samples SO 32/179, SO 39/181 and SO 39/188 all displayed similar IR spectral features (Figure 5). The strong adsorption at 3545–3555 cm^{-1}, as well as that at 816–818 cm^{-1} are associated with vibrations of the Fe^{3+}-Fe^{3+}-OH stretching. These adsorption bands indicate the Fe occupancy of the octahedral sites. The Si-O stretching adsorptions at 1017

https://doi.org/10.1346/CCMN.1994.0420605 Published online by Cambridge University Press

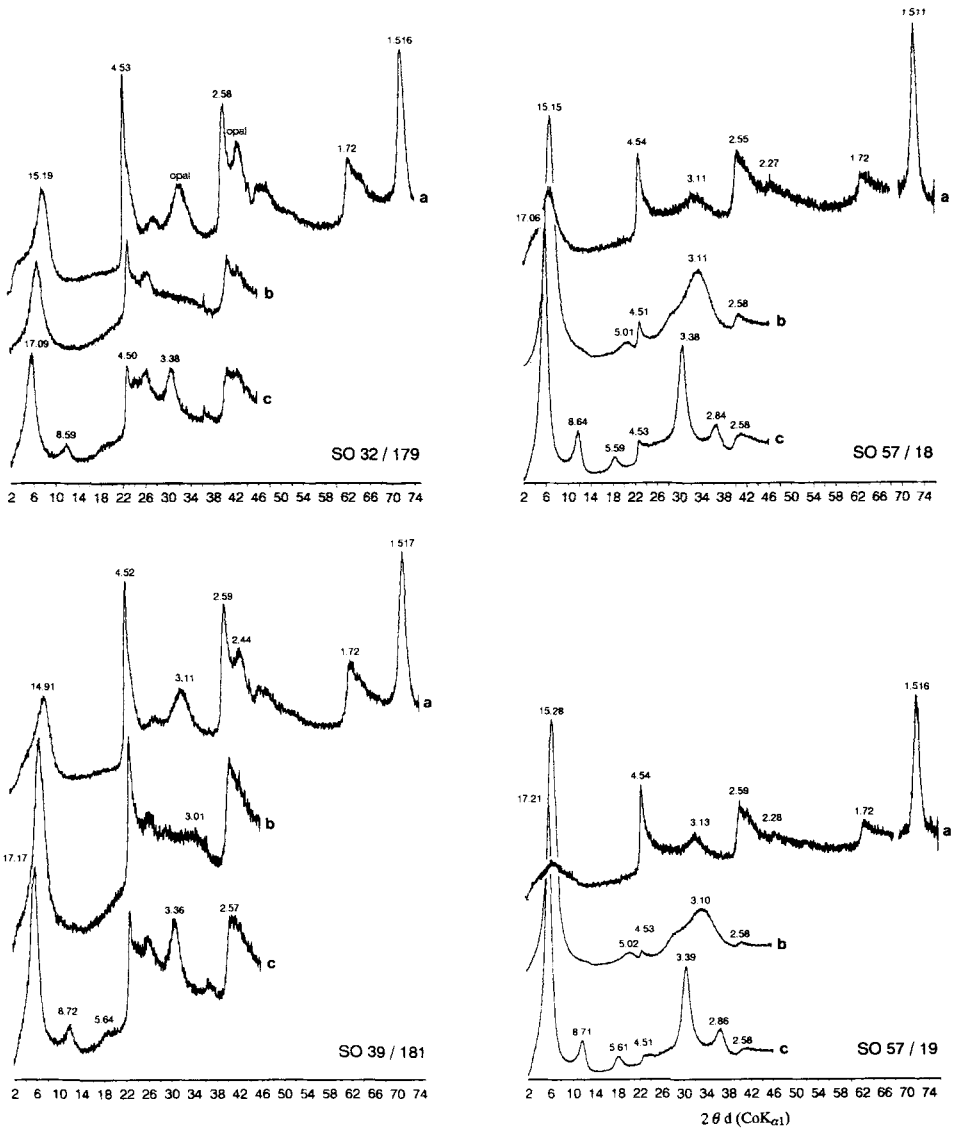

XRD

a bulk sample
unoriented, Mg–saturated
air–dried

b clay fraction (< 2 μm)
oriented, Mg–saturated
air-dried

c clay fraction (< 2 μm)
oriented, Mg–saturated
glycolated

https://doi.org/10.1346/CCMN.1994.0420605 Published online by Cambridge University Press

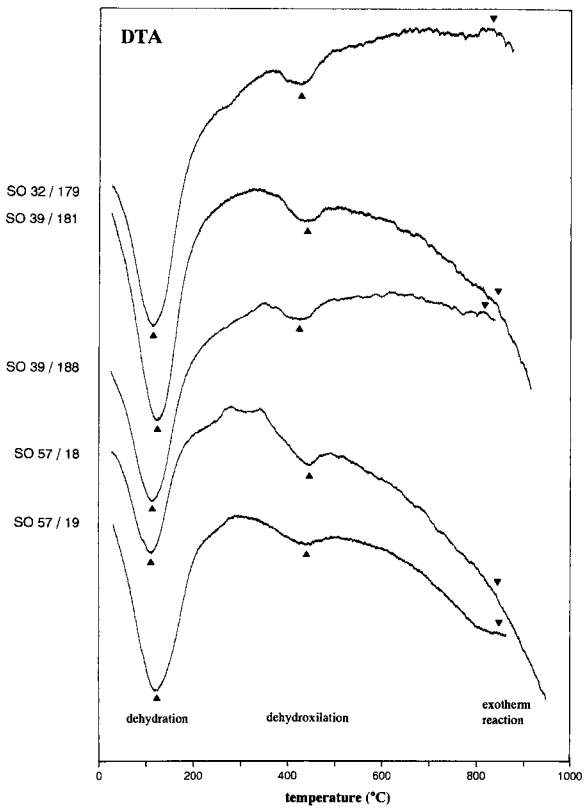

Figure 4. Differential thermal analysis (DTA) tracings of the clay fraction (<2 μm).

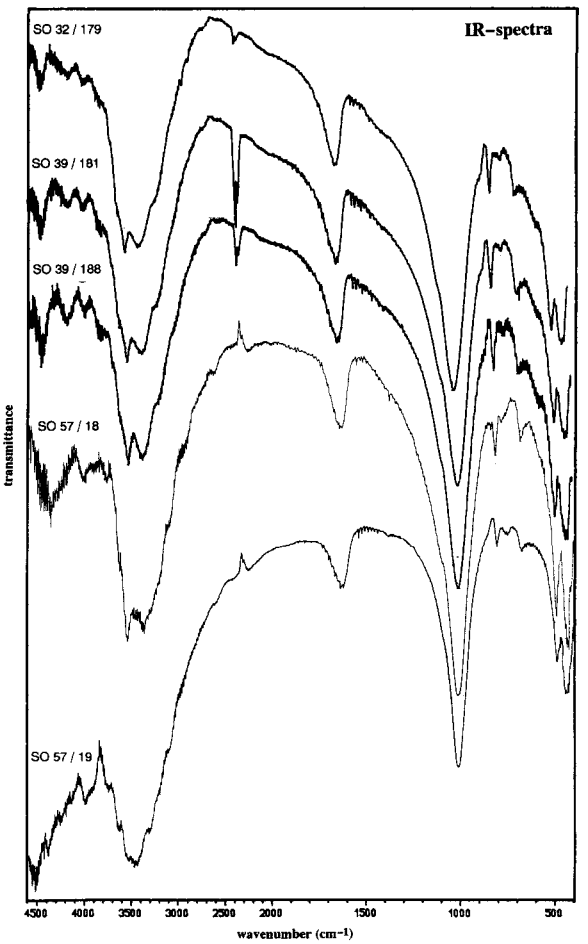

Figure 5. Infrared spectra of the Mg-saturated clay fractions (<2 μm).

cm^{-1} and 492–494 cm^{-1} suggest only minor substitution by Fe(III) in the tetrahedral layer. The IR spectra of the Mariana Trough clays were similar to those of the Galapagos Rift. The adsorption band at about 800 cm^{-1} indicates similar amounts of octahedral Mg^{2+}.

Transmission electron microscopy (TEM)

The dominant particle morphology of the Galapagos Rift and Mariana Trough clays is one of fine slightly folded sheets, less than 1 μm in diameter (Figures 6a and 6b). Sometimes the edges of the sheets are slightly rolled in or folded (Figures 6c and 6d). A less common form is that of weakly developed laths and fibers. The laths, with an average width of 0.1 μm, were also rolled along the edges (Figure 6f). In sample SO 32/179, the proportion of lath and fibrous particles was particularly large. Sometimes the margins of the sheets or laths appeared to disintegrate into fibers (Figure 6e).

Chemical composition

The major element concentrations of the fractions <2 μm are presented in Table 2. The major elements of the clay materials consisted of Si and Fe. Al contents were extremely low. This is consistent with the trend observed in many submarine hydrothermal nontronites. If adsorbed Mg is subtracted from total, Mg contents were also very low. The relatively low potassium contents indicated the absence of significant amounts of illitic layers. The exciding large ignition losses in samples SO 39/181 and SO 39/188 are probably due to organic matter. The samples from the Galapagos Rift appeared to be enriched in heavy metals as As and Zn. High Cu, As, and Zn concentration levels are reported by from this area of the Galapagos Rift.

Specific surface area

The specific surface area for Mariana Trough clays ranged from 862 m^2/g (SO 57/18) to 903 m^2/g (SO 57/19). They compared well with the values obtained for standard Manito, Washington, nontronite (884 m^2/g)

←

Figure 3. X-ray diffraction pattern ($CoK_{\alpha 1}$-radiation), peak numbers in Å; a) unoriented bulk sample, air-dried, Mg-saturated; c) oriented clay fraction (<2 μm), glycolated, Mg-saturated.

https://doi.org/10.1346/CCMN.1994.0420605 Published online by Cambridge University Press

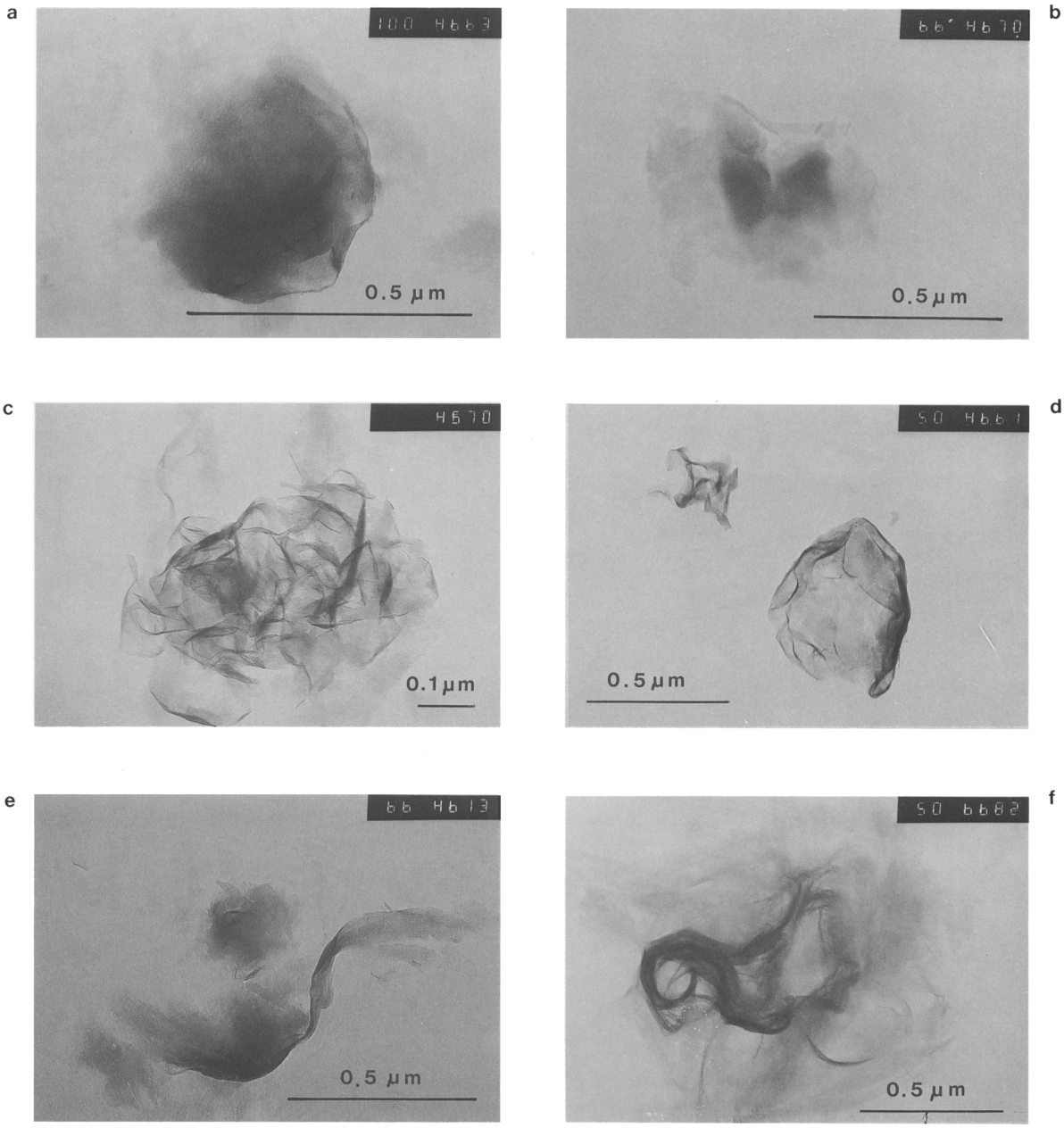

Figure 6. Transmission electron micrographs of the clay-fraction (<2 µm). a)–d) fine slightly folded sheet; e) sheet disintegrate into fibres; f) lath rolled and curled (the numbers in the right corner of the photographs represent the film numbers).

and Fe-rich smectite from Grant County, Washington (SWA-1) (882 m^2/g).

Oxygen isotope analysis

Oxygen isotope analysis was carried out from Mariana Trough materials, separately for the clay and for the opaline material. The formation temperatures calculated for the smectite of the Mariana Trough vary from 21.5° (26.3 $\delta^{18}O$) in sample SO 57/19 to 67.3°C (18.4 $\delta^{18}O$) in sample SO 57/18. With the opaline material of sample SO 57/19 a $\delta^{18}O$ of 31.2 was measured representing a calculated temperature of 28.4°C (minimum) to 44.0°C (maximum) (Botz and Stoffers 1992). The clay SO 32/179 from the Galapagos Rift yielded a formation temperature of 52°C (20.7 $\delta^{18}O$).

DISCUSSION

Submarine nontronites have repeatedly been described from near hydrothermal brine environments (see review in Chamley 1989).

https://doi.org/10.1346/CCMN.1994.0420605 Published online by Cambridge University Press

Table 2. Results of the chemical analysis of the clay fraction by XRF.

Sample	Fe_2O_3	SiO_2	Al_2O_3	MgO	MnO	Na_2O	K_2O	TiO_2	CaO	P_2O_5
					(weight %)					
SO 39/181	34.7	35.3	0.09	3.6	0.08	<	0.20	<	0.17	0.46
SO 39/188	31.1	29.0	0.07	3.5	0.12	<	0.30	<	0.14	0.37
SO 57/18	35.17	52.41	0.11	3.23	0.03	0.75	0.29	0.01	0.03	0.93
SO 57/19	30.75	52.37	0.28	6.03	0.06	0.18	0.15	0.03	0.05	1.74

Sample	SO_3	ZnO	As_2O_3	Sm_2O_3	GeO_2	V_2O_5	Cr_2O_3	Cl	LOI	Sum
					(weight %)					
SO 39/181	0.13	0.045	0.010	0.017	<	<	<	0.082	25.00	99.89
SO 39/188	0.10	0.092	0.010	0.011	0.014	<	<	0.052	35.00	99.88
SO 57/18	0.02	0.01	—	—	—	<	<	0.41	7.88	100.85
SO 57/19	0.03	0.01	—	—	—	<	<	0.76	8.97	100.64

— = not analysed, < = <100 ppm.

In their review of authigenic smectites in recent marine sediments, Cole and Shaw (1983) mention three modes of formation: alteration of volcanic rocks and glasses, low-temperature combination of biogenic silica and Fe-oxyhydroxides, and direct precipitation from hydrothermal fluids. This mechanism of direct precipitation has been proposed for the formation of authigenic nontronite in the hydrothermal field of the Galapagos Rift, where it occurs in mounds through which warm fluids (up to 30°C) percolate (Moorby and Cronan 1983, McMurtry *et al* 1983). Singer *et al* (1984) described a smectite close to the pure Fe endmember of the beidellite-nontronite series in the fine clay separated from a 354 cm long sediment core in the southwestern Pacific Basin. Oxygen isotope values determined on authigenic quartz, found in association with the nontronite, indicated a formation temperature of about 22°C. A similar formation temperature was also determined for a nontronite deposit from the Lau Basin, SW Pacific (Stoffers *et al* 1990). The arguments for the hydrothermal origin of the smoker-nontronites were based on the following features: (1) their purity and monomineralic character, (2) their extremely low Al content, (3) relatively low content of accessory minor elements, particularly Ba, and (4) their oxygen isotopic composition, which suggested relatively warm formation temperatures.

Table 3 gives the chemical composition of hydrothermal fluids as determined at various vents. Prominent are the very high Fe, Mn and Si concentrations in comparison to ambient sea water, particularly in the endmembers as calculated.

The contact of these rising acidic and reducing solutions with oxic sea water results in the precipitation of silicates, metal oxides, and hydroxides. The lower redox conditions required for the oxidation of Fe^{2+} compared to that of Mn^{2+} (Stumm and Morgan 1981) result in the precipitation of iron oxides closer to the vent, while Mn is transported further before precipitation.

Frequently, these precipitated oxides have been observed to exhibit a filamentous microstructure. Alt

Table 3. Composition of ambient seawater, seawater vent fluid mixtures, and vent fluids (calculated) for different ocean hydrothermal waters. Data from Karl *et al* 1988*, and Von Damm 1990**.

	East Pacific** Rise 21°N vent OBS	Southern** Juna de Fuca vent 1	Axial volcano** inferno	Hawaii, Loihi* Pele's Vent	Ambient seawater* 980 m near Pele's Vent
Temperature (°C)	350	285	149–328	30	3.5
pH	3.4	3.2	3.5	5.3–5.5	7.5
Na (mmol/kg)	432	661	500	464	455
Cl (mmol/kg)	489	896	625	524	534
Mg (mmol/kg)	0	0	0	50.3	52.2
SO_4 (mmol/kg)	0.50	−1.30	—	27	28.8
K (mmol/kg)	23.2	37.3	27.5	12.3	10.2
Ca (mmol/kg)	15.6	84.7	46.8	11.2	10.3
Si (μmol/kg)	822.6	1065.7	705.8	1285	123
Fe (μmol/kg)	960	10,349	1006	1010	0.05
Sr (μmol/kg)	81	230	—	88.5	86.9
Li (μmol/kg)	891	1108	637	36.5	23.6
Mn (μmol/kg)	960	2611	1081	21.1	0.01
Rb (μmol/kg)	28	28.0	—	2.85	1.25
Ba (μmol/kg)	>8	—	—	0.71	0.07
Al (μmol/kg)	5.2	—	—	—	—

https://doi.org/10.1346/CCMN.1994.0420605 Published online by Cambridge University Press

(1988) described it for amorphous Fe-oxyhydroxides, hematite and goethite from the Larson and Red Seamount, East Pacific Rise, Karl *et al* (1988) for iron oxides from Loihi Seamount, Hawaii, Juniper and Fouquet (1988) for Fe-oxides and opal-A from diverse hydrothermal sites in the East Pacific, Juan de Fuca and Explorer Ridge, and Stackelberg *et al* (1990) for Mn-oxides and Fe-silicates from the Lau Basin. Filamentous microstructures have also been observed for metal sulfides (Ag, Cu, Fe, Pb) in the Sea Cliff hydrothermal field of the northern Gorda Ridge, NE Pacific (Zierenberg and Schiffmann 1990).

Intensive explorations (by small submersibles) of various vent sites have established the presence of dense communities of bacteria and specialized macrofauna. For example Karl *et al* (1988) described thick, orange colored bacterial mats with iron oxide coatings that cover lava fields on the periphery of Loihi Seamount, Hawaii, active vents. Karl *et al* (1989) hypothesized that these bacteria may use ferrous iron as energy source. In the mixing zone between the oxic and anoxic marine environment the density of bacterial populations was estimated to be up to 10^7 cells per ml (Jannasch and Mottl 1985). Detailed descriptions of microbial populations associated with deep sea hydrothermal vents were given by Jannasch and Mottl (1985), Juniper and Fouquet (1988), and Tunnicliffe and Juniper (1990). In a study of oxide and nontronite deposits on seamounts in the East Pacific, Alt (1988) described long delicate filaments, about 1 μm in diameter, remarkably similar in morphology to genera of Fe oxidizing bacteria. The similarity was particularly striking for the sheath forming Sphaerotilus-Leptothrix and the Fe oxidizing strain of Metallogenium. Cowen *et al* (1986) and Alt (1988) suggested that bacteria were probably important in catalyzing the oxidation and precipitation of iron from hydrothermal fluids. Tunnicliffe and Fontaine (1987) described extra-cellular accumulations of hydroxides by sheathed bacteria that colonize the surfaces.

Moreover, silica precipitation too has been attributed to processes associated with the presence of bacteria. In an examination of a silica chimney near Philosophers vent on Explorer Ridge, NE Pacific, (and some other sites, too), Juniper and Fouquet (1988) observed branching filaments of iron oxide and amorphous silica (opal). The presence of organic matter and identifiable filamentous bacteria in one sample led the authors to suggest that both the iron and silica were deposited in association with filamentous microorganisms.

One of the unusual micromorphological features of the nontronite occurrences at the smokers is the frequent organization in form of microtubes. Though observed at different sites, the microtubes have very similar dimensions. While length is quite variable (being dependent on state of preservation and observation section) tube diameter and tube wall thickness are fairly uniform. This suggests the control by a factor that is independent of local conditions. The shape and dimensions of the nontronite microtubes, observed in the Galapagos and Mariana hydrothermal sites, match very closely those given for the sheath forming bacteria such as Leptothrix (Berthelin 1988). This suggests that Fe oxidizing bacteria had been involved in the formation of the smoker nontronites, too.

The synthesis experiments of Harder (1976, 1978) and Decarreau and Bonnin (1986) discussed above indicate that for nontronite precipitation very narrow concentration ranges of silica and very specific redox potential conditions are required. The nontronite layers appear inside the upper part of the vent channel and in contact to the vent channel outside the chimney. This is the mixing domain between the reduced hydrothermal solution and oxic seawater. The direct contact of these different phases could be expected to result in quick dilution and increase in the redox potential (Haymon and Kastner 1981), leading to Fe-oxyhydroxide and not to nontronite precipitation. In some parts of the samples SO 57/19 from the Mariana Trough a thin iron oxide crust is forming the intermediary layer between opal frame and nontronite. Nontronite formation, on the other hand, would be enhanced by the presence of a stabilizing, retarding factor that would limit dilution, and keep redox conditions stable for some time. Iron oxidizing, chemolithotrophic bacteria might very well have fulfilled this function. It can be envisaged that the passage of the solutions through the dense bacterial mats retarded dilution of the hydrothermal solutions by seawater. Moreover, it is also possible that metabolic activities of the microorganisms had, on a microscale range, an effect on the redox potential. The dilution of Si may have been sufficient to prevent supersaturation with regard to opal but not that of nontronite (Harder 1976, Singer *et al* 1984). According to Haymon and Kastner (1981) the effects of dilution on Si saturation counteract those of temperature decrease. Therefore, precipitation of silicates would require controlled cooling with minimal mixing. Also, assuming a pH of 5.6 and temperatures of 10°–15°C, as measured by Alt (1988) at the Red Seamount, the oxidation rate would be so slow that precipitation of massive Fe-oxyhydroxides would be prevented. Thus, any additional retardation of the mixing effect would be favorable for nontronite precipitation.

The likelihood for this biocatalytically induced nontronite precipitation process is increased if the advantages derived for the biological partner are recognized. These might be numerous, in analogy to smectite microorganism interaction in the terrestrial domain: the clay sheath might act (a) as a shield preventing overheating, rapid changes in solute flow rate or concentrations and in general preserving the microenvironment (Marshall 1968, 1969); and/or as a stabilizer of

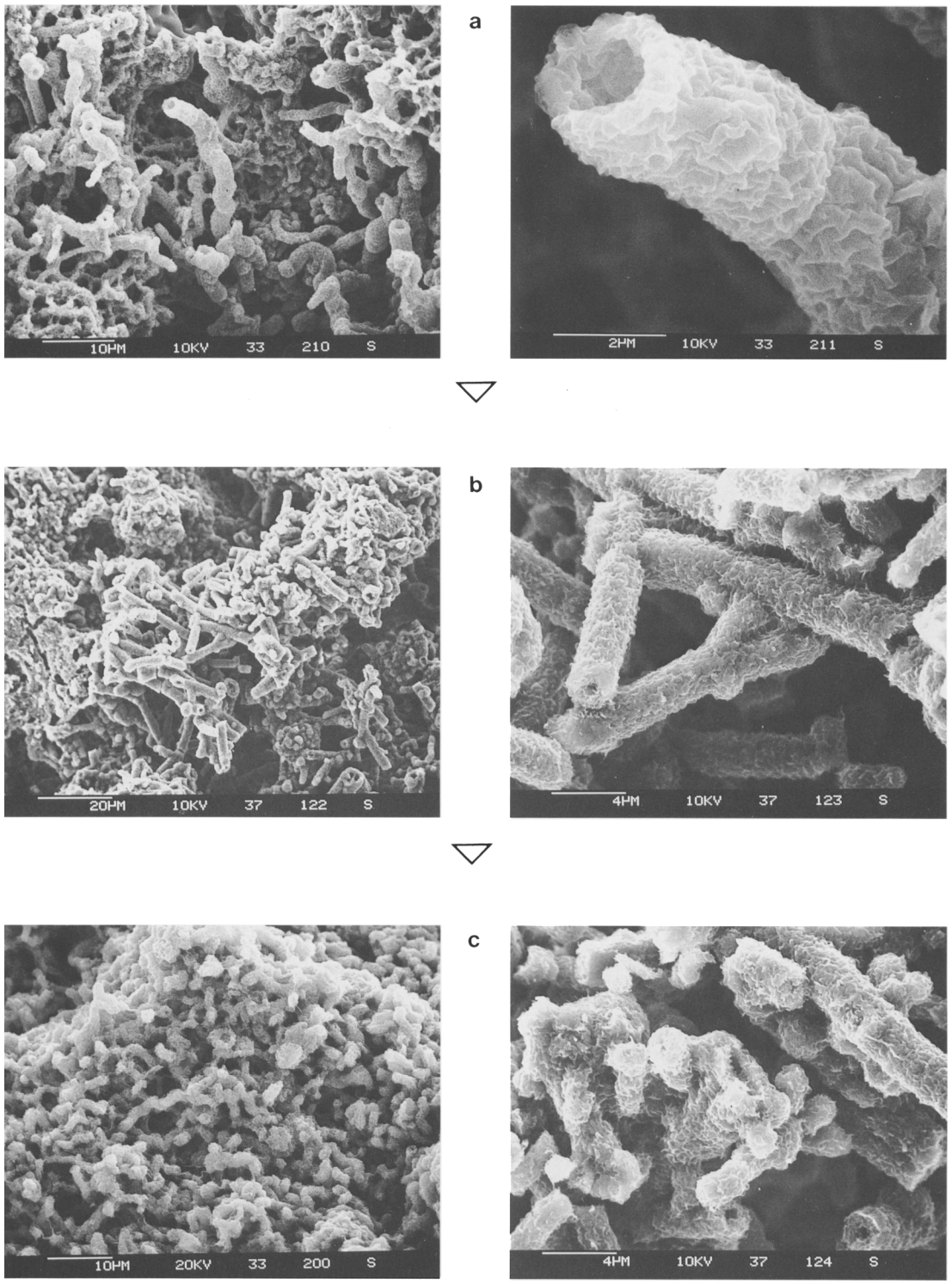

Figure 7. Degradation of microtubes with a secondary intergrowth of nontronite (SEM observations).

https://doi.org/10.1346/CCMN.1994.0420605 Published online by Cambridge University Press

pH conditions in a range favorable for the microorganism against strong fluctuation (Stotzky 1966; Stotzky and Rem 1966); (b) as a stimulation of metabolic activity (Marshall 1971; Ehrlich 1981); (c) as a regulation of the release of inorganic and organic nutrients (retained as exchangeable cations in the clay material) (Ehrlich 1981); and/or as inactivation mechanism of toxic substances by the cation exchange mechanism of the clay (Filip 1979).

The first biocatalytically induced nontronite crystallites formed might have served as crystallization nucleii for additional precipitation.

Alt (1988) observed a close relation between smoker activity and the formation of such mineralized microtubes. Well formed microtubes are associated with active smokers whereas at inactive chimneys the tubes are mechanically disturbed and altered by secondary crystallization. This corresponds to the activity of the bacteria population, which can only survive at active smokers. Observation of nontronite in different chimneys or parts of it suggested a degradation and secondary intergrowth of the nontronite tubes accompaneys or parts of it suggested a degradation and secondary intergrowth of the nontronite tubes accompanying the deactivation of the chimney (Figure 7).

CONCLUSIONS

Nontronite, in association with Fe-oxyhydroxides and amorphous silica, is found on the outer and inner walls of vent chimneys in silicate smokers.

Micromorphology, chemical composition and oxygen isotope data indicate that the nontronite is authigenic and had formed from the iron and silica present in the hydrothermal vent solutions.

The distinct microtube-like morphology of the nontronite clay aggregates suggests that sheath forming, Fe oxidizing bacteria play a decisive role in nontronite formation.

ACKNOWLEDGMENTS

The support given by the Deutsche Forschungsgemeinschaft (DFG) to the authors from the Federal Republic of Germany is gratefully acknowledged. For analytical help and comments we thank N. Bahat (TEM), E. Ben-Dor (specific surface area), Dr. H. Rozen, Prof. Dr. L. Margulies (IR), and Dr. D. Szafranek (SEM) from the Hebrew University and Dr. C. Samtleben (SEM), Dr. R. Botz (O-isotope), Dr. H. Lange (XRD), U. Schuldt, and Perbanth (photographs) from the Kiel University.

REFERENCES

Alt, J. C. 1988. Hydrothermal oxide and nontronite deposits on seamounts in the eastern Pacific. *Mar. Geol.* **81**: 227–239.

Badaut, D., G. Besson, A. S. Decarreau, and R. Rautureau. 1985. Occurrence of a ferrous, trioctahedral smectite in recent sediments of Atlantis II Deep, Red Sea. *Clay Miner.* **20**: 389–404.

Badaut, D., G. Blanc, and A. Decarreau. 1990. Variation des minéraux argileux ferrifères, en fonction du temps et de l'espace, dans les dépôts métallifères de la fosse Atlantis II en Mer Rouge. *C.R. Acad. Sci. Paris* **310**: 1069–1075.

Badaut, D., A. Decarreau, and G. Besson. 1992. Ferripyrophyllite and related Fe^{3+} rich 2:1 clays in recent deposits of Atlantis II Deep, Red Sea. *Clay Miner.* **27**: 227–244.

Berthelin, J. 1988. Microbial weathering processes in natural environments. In *Physical and Chemical Weathering in Geochemical Cycles.* A. Lerman and M. Meybeck, eds. NATO ASI Series C **251**: 33–59.

Bischoff, J. L. 1972. A ferroan nontronite from the Red Sea geothermal system. *Clays & Clay Miner.* **20**: 217–223.

Borthwick, J., and R. S. Harmon. 1982. A note regarding ClF_3 as an alternative to BrF_5 for oxygen isotope analysis. *Geochim. Cosmochim. Acta* **46**: 1665–1668.

Botz, R., and P. Stoffers. 1992. Isotopic composition of hydrothermal precipitates from the Mariana Trough. *Mar. Geol.* **108**: 239–245.

Carter, D. L., M. D. Heilmann, and C. L. Gonzales. 1965. Ethylene glycol monoethyl ether for determining surface area of silicate minerals. *Soil Science* **100**: 356–360.

Chamley, H. 1989. *Clay Sedimentology.* Berlin: Springer.

Clayton, R. N., J. R. O'Neil, and T. K. Mayeda. 1972. Oxygen isotope exchange between quartz and water. *J. Geophys. Res.* **77**: 3057–3067.

Cole, T. G. 1983. Oxygen isotope geothermometry and origin of smectites in the Atlantis II Deep, Red Sea. *Earth Planet. Sci. Lett.* **66**: 166–176.

Cole, T. G. 1985. Composition, oxygen isotope geochemistry, and origin of smectite in the metalliferous sediments of the Bauer Deep, southeast Pacific. *Geochim. Cosmochim. Acta* **49**: 221–235.

Cole, T. G., and H. F. Shaw. 1983. The nature and origin of authigenic smectites in some recent marine sediments. *Clay Miner.* **18**: 239–252.

Corliss, J. B., J. Dymond, L. I. Gordon, J. M. Edmond, R. P. von Herzen, and R. D. Ballard. 1979. Submarine thermal springs on the Galapagos Rift. *Science* **203**: 1073–1083.

Cowen, J. P., G. J. Massoth, and E. T. Baker. 1986. Bacterial scavenging on Mn and Fe in a mid- to far-field hydrothermal particle plume. *Nature* **322**: 169–171.

Decarreau, A., and D. Bonnin. 1986. Synthesis and crystallogenesis at low temperature of Fe(III)-smectites by evolution of coprecipitated gels: Experiments in partially reducing conditions. *Clay Miner.* **21**: 181–194.

Decarreau, A., D. Bonnin, D. Badaut-Trauth, and R. Couty. 1987. Synthesis and crystallogenesis of ferric smectite by evolution of Si-Fe coprecipitates in oxidizing conditions. *Clay Miner.* **22**: 207–223.

Edmond, J. M., C. Measures, B. Mangun, B. Grant, F. R. Sclater, R. Collier, A. Hudson, L. I. Gordon, and J. B. Corliss. 1979. On the formation of metal-rich deposits at ridge crests. *Earth Planet. Sci. Lett.* **46**: 19–30.

Edmond, J. M., K. L. Von Damm, R. E. McDuff, and C. I. Measures. 1982. Chemistry of hot springs on the East Pacific Rise and their effluent dispersal. *Nature* **297**: 187–191.

Ehrlich, H. L. 1981. *Geomicrobiology.* New York: Marcel Dekker.

Filip, Z. 1979. Wechselwirkungen von Mikroorganismen und Tonmineralen—eine Übersicht. *Zeitschrift für Pflanzenernährung und Bodenkunde* **142**: 375–386.

Harder, H. 1976. Nontronite synthesis at low temperatures. *Chem. Geol.* **18**: 169–180.

Harder, H. 1978. Synthesis of iron layer silicate minerals under natural conditions. *Clays & Clay Miner.* **26**: 65–72.

Haymon, R. M. 1983. Growth history of hydrothermal black smoker chimneys. *Nature* **301**: 695–698.

Haymon, R. M., D. J. Fornari, K. L. von Damm, M. D. Lilley, M. R. Perfit, J. M. Edmond, W. C. Shanks III, R. A. Lutz, J. M. Grebmeier, S. Carbotte, D. Wright, E. McLaughlin, M. Smith, N. Beedle, and E. Olson. 1993. Volcanic eruption of the mid-ocean ridge along the East Pacific Rise at 9°45–52′N: Direct submersible observations of seafloor phenomena associated with an eruption event in April, 1991. *Earth Planet. Sci. Lett.* **119**: 85–101.

Haymon, R. M., and M. Kastner. 1981. Hot spring deposits on the East Pacific rise at 21°N: preliminary description of mineralogy and genesis. *Earth Planet. Sci. Lett.* **53**: 363–381.

Haymon, R. M., and K. C. MacDonald. 1985. The geology of deep-sea hot springs. *American Scientist* **73**: 441–449.

Heath, G. R., and J. Dymond. 1977. Genesis and transformation of metalliferous sediments from the East Pacific Rise, Bauer Deep, and Central Basin, northwest Nazca plate. *Geol. Soc. Am. Bull.* **88**: 723–733.

Jannasch, H. W., and M. J. Mottl. 1985. Geomicrobiology of deep-sea hydrothermal vents. *Science* **229**: 717–725.

Juniper, S. K., and Y. Fouquet. 1988. Filamentous iron-silica deposits from modern and ancient hydrothermal sites. *Can. Mineral.* **26**: 859–869.

Karl, D. M., A. M. Brittain, and B. D. Tillbrook. 1989. Hydrothermal and microbial processes at Loihi Seamount, a mid-plate hot spot volcano. *Deep-Sea Res.* **36**: 1655–1673.

Karl, D. M., G. M. McMurtry, A. Malahoff, and M. O. Garcia. 1988. Loihi Seamount, Hawaii: A mid-plate volcano with a distinctive hydrothermal system. *Nature* **335**: 532–535.

Knauth, L. P., and S. Epstein. 1976. Hydrogen and oxygen isotope ratios in nodular and bedded cherts. *Geochim. Cosmochim. Acta* **40**: 1095–1108.

Köhler, B. 1991. Eigenschaften und Genese von marinen, authigenen Smektiten aus aktiven Hydrohthermalgebieten. *Berichte-Reports, Geol.-Paläont. Inst. Univ. Kiel* **47**: 111 pp.

Köhler, B., and A. Singer. 1992. A marine hydrothermal nontronite modification at smoker chimneys. A bacteria-influenced formation?. *Zbl. Geol. Paläont. Teil I* **5**: 407–414.

MacDonald, K. C., K. Becker, F. N. Spiess, and R. D. Ballard. 1980. Hydrothermal heat flux of the "black smoker" vents on the East Pacific Rise. *Earth Planet. Sci. Lett.* **48**: 1–7.

Marshall, K. C. 1968. Interaction between colloidal montmorillonite and cells of rhizobium species with different ionogenic surfaces. *Biochim. Biophys. Acta* **156**: 179–186.

Marshall, K. C. 1969. Studies by microelectrophoretic and microscopic techniques of the sorption of illite and montmorillonite to rhizobia. *J. Gen. Microbiol.* **56**: 301–306.

Marshall, K. C. 1971. Sorptive interactions between soil particles and microorganisms. In *Soil Biochemistry 2.* A. D. McLaren and J. Skujins, eds. New York: Marcel Dekker, 409–445.

McMurtry, G. M., C.-H. Wang, and H.-W. Yeh. 1983. Chemical and isotopic investigations into the origin of clay minerals from the Galapagos hydrothermal mounds field. *Geochim. Cosmochim. Acta* **47**: 475–489.

Mehra, O. P., and M. L. Jackson. 1960. Iron oxide removal from soils and clays by a dithionite-citrate system buffered with sodium bicarbonate. *Clays & Clay Miner.* **7**: 317–327.

Moorby, S. A., and D. S. Cronan. 1983. The geochemistry of hydrothermal and pelagic sediments from the Galapagos hydrothermal mounds field, D.S.D.P. Leg 70. *Mineral Mag.* **47**: 291–300.

Rona, P. A. 1984. Hydrothermal mineralization at seafloor spreading centers. *Earth-Science Reviews* **20**: 1–104.

Singer, A., and P. Stoffers. 1987. Mineralogy of a hydrothermal sequence in a core from the Atlantis II Deep, Red Sea. *Clay Miner.* **22**: 251–267.

Singer, A., P. Stoffers, L. Heller-Kallai, and D. Szafranek. 1984. Nontronite in a deep-sea core from the South Pacific. *Clays & Clay Miner.* **32**: 375–383.

Spiess, F. N., K. C. MacDonald, T. Atwater, R. Ballard, A. Carranza, D. Cordoba, C. Cox, V. M. Diaz Garcia, J. Franchetau, J. Guerrero, J. Hawkins, R. Haymon, R. Hessler, T. Juteau, M. Kastner, R. Larson, C. Luyendyk, J. D. MacDougall, S. Miller, W. Mormark, J. Orcutt, and C. Rangin (RISE Project group). 1980. East Pacific Rise: Hot springs and geophysical experiments. *Science* **207**: 1421–1433.

Stackelberg, U. von, V. Marchig, P. Müller, and T. Weiser. 1990. Hydrothermal mineralization in the Lau and North Fiji Basins. *Geol. Jb.* **D 92**: 547–614.

Stoffers, P., R. Botz, J. L. Cheminée, C. W. Devey, V. Frogler, G. P. Glasby, M. Hartmann, R. Hekinian, F. Kögler, D. Laschek, P. Larqué, W. Michaelis, R. K. Mühe, D. M. Puteanus, and H. H. Richnow. 1989. Geology of Macdonald Seamount Region, Austral Islands: Recent hotspot volcanism in the South Pacific. *Mar. Geophys. Res.* **11**: 101–112.

Stoffers, P., A. Singer, G. M. McMurtry, A. Arquit, and H.-W. Yeh. 1990. Geochemistry of a hydrothermal nontronite deposit from the Lau basin, Southwest Pacific. *Geol. Jb.* **D 92**: 615–628.

Stotzky, G. 1966a. Influence of clay minerals on microorganisms: II. Effect of various clay species, homoionic clays, and other particles on bacteria. *Can. J. Microbiol.* **12**: 831–848.

Stotzky, G. 1966b. Influence of clay minerals on microorganisms. III. Effect of particle size, cation exchange capacity, and surface area on bacteria. *Can. J. Microbiol.* **12**: 1235–1246.

Stotzky, G., and L. T. Rem. 1966. Influence of clay minerals on microorganisms. I. Montmorillonite and kaolinite on bacteria. *Can. J. Microbiol.* **12**: 547–563.

Stumm, W., and J. J. Morgan. 1981. *Aquatic Chemistry.* New York: Wiley.

Tunnicliffe, V., M. Botros, M. E. de Burgh, A. Dinet, H. P. Johnson, S. K. Juniper, and R. E. McDuff. 1986. Hydrothermal vents of Explorer Ridge, northeast Pacific. *Deep-Sea Res.* **33**: 401-412.

Tunnicliffe, V., and A. R. Fontaine. 1987. Faunal composition and organic surface encrustations at hydrothermal vents on the southern Juan de Fuca Ridge. *J. Geophys. Res.* **33**: 303–311.

Tunnicliffe, V., and S. K. Juniper. 1990. Dynamic character of the hydrothermal vent habitat and the nature of sulphide chimney fauna. *Progress in Oceanography* **24**: 1–13.

Von Damm, K. L. 1990. Seafloor hydrothermal activity: Black smoker chemistry and chimneys. *Annu. Rev. Earth Planet. Sci.* **18**: 173–204.

Weiss, R. F., P. Lonsdale, J. E. Lupton, A. E. Bainbridge, and H. Craig. 1977. Hydrothermal plumes in the Galapagos Rift. *Nature* **267**: 600–603.

Yeh, H. W., and S. M. Savin. 1977. Mechanism of burial metamorphism of argillaceous sediments: 3. O-isotope evidence. *Geol. Soc. Am. Bull.* **88**: 1321–1330.

Zierenberg, R. A., and P. Schiffmann. 1990. Microbial control of silver mineralization at a sea-floor hydrothermal site on the northern Gorda Ridge. *Nature* **348**: 155–157.

(Received 3 November 1993; accepted 4 June 1994; Ms. 2437)